

Calogero-Sutherland-Lieb-Liniger gas in one-dimensional cold atoms

Yue Yu

Institute of Theoretical Physics, Chinese Academy of Sciences, P.O. Box 2735, Beijing 100080, China

(Dated: February 1, 2022)

We study an array of cigar-like Bose atom condensates confined in a cylinder and examine the competition between the dipole-dipole and the short range interactions. The system is effectively reduced to a one-dimensional boson one with a contact and inverse square interactions. We call this system the Calogero-Sutherland-Lieb-Liniger gas. The universal properties of the ground state are analyzed by the renormalization group theory. By using the bosonization techniques to the exclusion gas, we calculate the non-universal exponent depending on the microscopic parameters. This exponent may be experimentally measurable.

PACS numbers: 03.75.Lm, 67.40.-w, 39.25.+k

One-dimensional many-particle systems have been a central topics in physics for four decades. Many exactly soluble models were proposed after Bethe solved the one-dimensional Heisenberg model by his famous ansatz [1, 2]. Among them two kinds of the exactly models are cross-sectional: The particles interacting with contact [3] or with inverse square potentials [4, 5]. The one-dimensional cold alkali metal Bose atom gas, which may condense at zero temperature [6], is a typical example of the former. Here, we call it the Lieb-Liniger (L-L) gas for Lieb and Liniger first gave the exact solution for this model. The strong interacting limit of the L-L model, known as the Tonks-Girardeau (T-G) gas [7], has also reached in the ultracold Bose atoms [8]. The model with inverse square interaction, called the Calogero-Sutherland (C-S) models play a fundamental role in the contemporary theoretical physics [9]. The C-S model may be a universal Hamiltonian of some weakly disordered metals [10]. The models may also be used to describe the edge excitations in the fractional quantum Hall effect [11]. In a recent work [12], we proposed a possible realization of the C-S gas for the cold atom with a dipole-dipole interaction, which is based on a major progress in the cold chromium atoms ^{52}Cr i.e., this cold atom gas is turned into a Bose condensate [13]. It may also be realizable in the cold atom in tight waveguides with anyonic exchange symmetry [14].

The models with both the short range and long range interactions mentioned above have been applied to the faceting transition of the miscut crystal surface [15, 16] by renormalization group analysis [17]. The low energy effective theory of these models may be characterized by the non-ideal exclusion gas [18] since the quasi-particle excitations in these models obey exclusion statistics [19, 20, 21]. It is a Luttinger liquid theory [22, 23] whose non-universal exponent is given by both the short range interaction strength and the exclusion statistics parameter.

Both interactions are of the comparative magnitude in the cold chromium atom gas [13]. This offers an opportunity to study the intergradation from one to another since both interactions are adjustable [24, 25]. In this Letter, we propose a realization of such a model for the

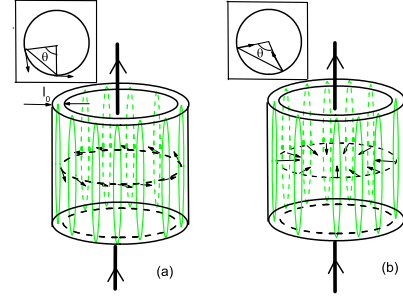


FIG. 1: (Color on-line) The cigar-like condensates are confined in a cylinder. (a) The magnetic dipoles; (b) The electric dipoles. The insets show the angle relation in deriving eq. (2)

cold atoms in a cylinder. Fig. 1 is a sketch map of our set up. An array of cigar-like Bose atom condensates is confined in a cylinder which is made by, e.g., a ring-shaped optical lattice [26]. The atoms interact with a contact potential accompanied a dipole-dipole potential [27]. An electromagnetic field is generated by a stable current. If the dipoles is magnetic, their orientations are shown in Fig. 1(a) while the orientations are as in Fig. 1(b) if they are electric. The arc coordinate is x and the vertical direction is y . The two-dimensional wave function of the many atom system is factorized, i.e., the y -direction wave function is approximated by its condensate wave function and the system effectively is one-dimensional. The effective atom density of the system may be written as $\rho(\mathbf{r}) = \rho_0(y) \sum_{i=1}^N \delta(x-x_i)$ where $\rho_0(y)$, approximated by a constant ρ_0 , is the atom density in a single cigar-like condensate and N the number of the condensates.

The three-dimensional interacting potential of the atom cloud is generally given by $V = \frac{1}{2} \int_S d\mathbf{r} d\mathbf{r}' \rho(\mathbf{r}) V(\mathbf{r} - \mathbf{r}') \rho(\mathbf{r}')$ where S denotes the cylinder with the thick l_0 . For simplicity, we consider a dilute gas limit in which whatever an optical lattice exists, the continuous model works. The dilute condition is given by $r_0 N/L \ll 1$ where L is the perimeter of the circle and r_0 is the az-

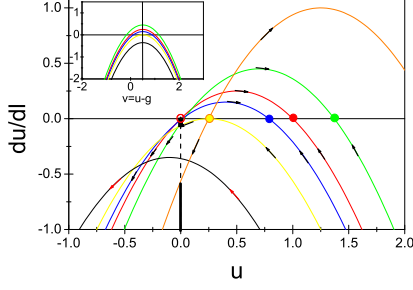


FIG. 2: (Color on-line) The renormalization group flows for $g=0.75$ (orange), 0.2 (green), 0 (red), -0.1 (blue), -0.25 (yellow) and -0.6 (black). The arrows show the flow directions. The filled spots are the stable fixed points and the empty are the unstable fixed points.

imathal width of a condensate. The interaction $V(\mathbf{r}_{ij} = \mathbf{r}_i - \mathbf{r}'_j)$ consists of two parts

$$V = \sum_{i<j} \left[U\delta(\mathbf{r}_{ij}) + \frac{\mathbf{d}_i \cdot \mathbf{d}_j - 3(\mathbf{d}_i \cdot \hat{\mathbf{r}}_{ij})(\mathbf{d}_j \cdot \hat{\mathbf{r}}_{ij})}{r_{ij}^3} \right], \quad (1)$$

where $U = \frac{4\pi\hbar^2 a}{m}$ for a is the s -wave scattering length. \mathbf{d} is the dipolar moment of the atom. For the factorized wave function, the Hamiltonian may be reduced to a one-dimensional one

$$H_1 = -\sum_{i=1}^N \frac{\hbar^2}{2m} \frac{d^2}{dx_i^2} + U_1 \sum_{i<j} \delta_{r_c}(x_{ij}) \quad (2)$$

$$+ \frac{G\pi^2}{L^2} \sum_{i<j} \sin^{-2} \frac{\pi(x_i - x_j)}{L} - \delta_{\pm} \frac{g\pi^2}{L^2} N(N-1)$$

where $G = 2d^2\rho_0$, $U_1 \propto \frac{\hbar^2 a}{m l_0 r_0}$ is the one-dimensional reduction of U , whose detailed version depends on the constraint potential. $r_c \rightarrow 0$ is the character size of the contact potential. $\delta_{\pm} = \frac{1 \pm 2}{2}$ and the sign \mp corresponds to the magnetic or electric dipoles in Fig.1(a) or (b). The δ_{\pm} term in the Hamiltonian is not important in the thermodynamic limit because it is of order $O(1)$ while the ground state energy of the system is an extended quantity. We call this system the L-L-C-S gas since it combines the C-S and L-L gases. In the following, we use the dimensionless coupling constants $g = \frac{m}{\hbar^2} G$, $u = \frac{m r_c}{\pi \hbar^2} U_1$, and $v = u - g$ with r_c/l_0 fixed when r_c and $l_0 \rightarrow 0$. In the system our are concerning, $g \geq 0$ while u may be a real number.

To understand the universal properties of the ground state, we employ the renormalization group theory. This has been built for models with both contact and long range interactions [17]. For this inverse square model in the one-dimension, the renormalization group equation reads

$$\frac{du}{dl} = (2g+1)u - u^2 - g^2, \text{ or } \frac{dv}{dl} = v - v^2 + g \quad (3)$$

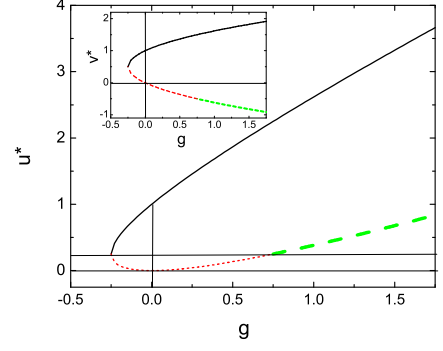


FIG. 3: (Color on-line) The fixed point lines. The solid(black) curve is the stable fixed points. In the red curves a pair of different g are corresponding to the same unstable fixed point u^* . And in the green, the unstable fixed point for $g > 0.75$ shares the same u^* with the stable fixed point.

while the long range coupling constant g is a marginal operator. Here $l = \ln N$ is the running parameter. The flow pattern $\frac{dv}{dl}$ and the fixed point values v^* are shown in the insets of Fig. 2 and Fig. 3, respectively [15, 17]. Since $g \geq 0$ in the present model, one may write $g = \lambda(\lambda - 1)$ for a real λ . The fixed point value v^* for a given g equals to λ . In a pure C-S model, it is known that λ serves as the exclusion statistics parameter[21]. This means that the fixed point line of this model is determined by exclusion statistics of the system. To understand the physics directly from the microscopic parameters, we redraw the flow and fixed point line in $u - \frac{du}{dl}$ and $g - u^*$ in Fig. 2 and Fig. 3, respectively. In Fig. 2, we see that there are two fixed points in a flow line for a given $g > -0.25$. The right hand side one is stable and the left one is unstable. Each fixed point value u^* corresponds to two $g_{\pm} = u^* \pm \sqrt{u^*}$. If $0 < u^* < 0.25$, both fixed points are unstable. For $u^* > 0.25$, one of g_+ is unstable while g_- 's is stable. Fig. 3 clearly shows this fact. It is seen that there is no fixed point with $u^* < 0$ or $g < -0.25$. If $g < -0.25$, the attraction between condensates (called particles hereafter) is so strong that the on-site repulsion can not withstand the collapse. This collapse, however, will not happen for the system we are considering, in which $g > 0$.

If we only concentrate on the short range interaction, the above renormalization group analysis for the ground state properties may be complete. However, since the long range interaction may lead to consequences with the exception of the above renormalization group analysis, we have to carefully examine the ground state. The renormalization group flows show that the pure C-S model with $u = 0$ is driven to $u \rightarrow -\infty$. We examine the meaning of this running now. There are two real solutions for $g = \lambda(\lambda - 1)$ if $g > -0.25$, i.e., $\lambda_{\pm} = 0.5(1 \pm \sqrt{1+4g})$. The ground state energy is given by [5] $E_{\lambda} = \frac{\pi^2 \lambda^2}{L^2} \sum_{j=1}^N (2j - N - 1)^2$. For $-0.25 < g < 0$,

$0 < \lambda_- < 0.5$ and the ground state wave function of the C-S model is given by

$$\Psi_{C-S} = \prod_{i < j} \left[\sin \frac{\pi(x_i - x_j)}{L} \right]^{\lambda_-}. \quad (4)$$

This means that although the interaction is attractive, there is still a mutual repulsion between particles caused by the quantum zero motion such that the system is still stable against the collapse. Since the contact potential is less singular than the $1/x^2$ potential, for $-0.25 < g < 0$, no matter what is the magnitude of u , the ground state wave function exactly given by (4). Reflected in Fig. 2, there is a small region between the red curve and the yellow curve at $u = 0$ (the black short stub), the system may be characterized by the C-S model. We have discussed such a situation in our previous work [12] and do not concern it here because in our model $g > 0$.

For $g > 0.75$, $\lambda_- < -0.5$, and (4) is not square integrable, the ground state wave function is given by [5]

$$\Psi_{C-S} = \prod_{i < j} \left[\sin \frac{\pi(x_i - x_j)}{L} \right]^{\lambda_+}, \quad (5)$$

with $\lambda_+ > 1.5$. Hence, the system will not run to $u = -\infty$ from the unstable fixed points but is characterized by the thick vertical line at $u = 0$ in Fig. 2.

For $0 < g < 0.75$ ($-0.5 < \lambda_- < 0$), there is a ground state (4) which is square integrable. The renormalization group flow indeed will drive the system to a state with $u = -\infty$ for a negative u fluctuation. However, at exact $u = 0$, because of the symmetry $\lambda \leftrightarrow -\lambda$ [28][16], the system is equivalent to that with $0 < \lambda < 0.5$. This character of the system is shown by the vertical dash line in Fig. 2.

According to the above analysis, we have an overall view to the ground states of the system. We see that there is no ground state with $0.5 < \lambda < 1.5$ in the present model. This is because the non-interaction particles are boson, the system has to back to the free boson when $g = u = 0$. If applying this model to fermions, λ_- solutions have to be abandoned because $\lambda \rightarrow 1$ as $g \rightarrow 0$.

In the cold atom context, many system parameters may be exactly controlled. Therefore, one should do microscopic calculations to understand many non-universal properties. Here we use an effective theory early developed in [18], to study some low energy behaviors of the system. The theory was called the exclusion gas theory. Due to the symmetry $\lambda \leftrightarrow -\lambda$, we focus on $\lambda \geq 0$.

We first consider $\lambda \neq 0$. The pseudo-Fermi-momentum is defined by $k_F \equiv \sqrt{2m\mu}$ for the chemical potential μ . Its value is fixed by $\int_{-k_F}^{k_F} dk \rho(k) = \frac{N_0}{L} \equiv \bar{d}_0$ for N_0 is the one-dimensional particle number in the ground state. The particle density $\rho(k) = 1/(2\pi\hbar)$ if $|k| < k_F$ and 0 if $|k| > k_F$. This gives $k_F = \pi\lambda\hbar\bar{d}_0$ and $\mu = \frac{1}{2m}(\pi\lambda\hbar\bar{d}_0)^2$. The ground state energy can be written as, in the thermodynamic limit, $E_\lambda/L = \frac{1}{2m} \int_{-k_F}^{k_F} dk \rho(k) k^2 = \frac{\hbar^2}{6m} \pi^2 \lambda^2 \bar{d}_0^3$.

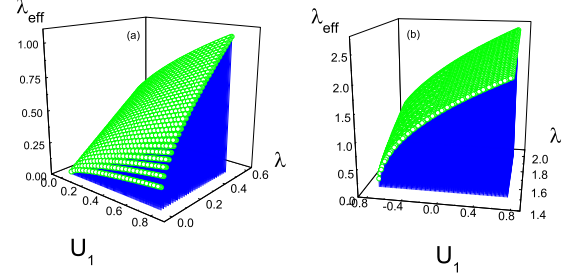


FIG. 4: (Color on-line) The effective Luttinger liquid parameter λ_{eff} (the green surfaces) varies as λ and U_1 . The unit of U_1 is $\hbar v_s$. (a) $0 < \lambda < 0.5$; (b) $\lambda > 1.5$.

the low-lying excitations of the system are: The density fluctuations with the sound velocity $v_s = v_F = k_F/m$; Adding extra number $M = N - N_0$ of particles to the ground state; And creating a persist current by the Galileo boost $k \rightarrow k + \pi\hbar/L$ in the ground state. To obey the periodic condition, one requires $(-1)^J = (-1)^M$ for integers M and J . If we consider only these low-lying excitations, the non-ideal exclusion gas may be described by a bosonized effective Hamiltonian [18]

$$\begin{aligned} H_B = & \frac{1}{2} \sum_{q>0} q \left[(v_s + U_1/\hbar) (b_q^\dagger b_q + \tilde{b}_q^\dagger \tilde{b}_q + b_q b_q^\dagger + \tilde{b}_q \tilde{b}_q^\dagger) \right. \\ & + (U_1/\hbar) (b_q^\dagger \tilde{b}_q^\dagger + b_q \tilde{b}_q + \tilde{b}_q^\dagger b_q^\dagger + \tilde{b}_q b_q) \left. \right] \\ & + \frac{\pi}{L} [U_1 (M_R^2 + M_L^2) + 2U_1 M_R M_L] \\ & + \frac{\hbar}{2} \frac{\pi}{L} [v_N M^2 + v_J J^2], \end{aligned} \quad (6)$$

where $v_N = \lambda v_s$ and $v_J = v_s/\lambda$ are the standard Luttinger liquid relation [22]. The boson operators b_q and \tilde{b}_q are related to the density fluctuating operators $\rho_q^{(\pm)}$ by $b_q = \sqrt{2\pi/qL} \rho_q^{(+)}$, $\tilde{b}_q = \sqrt{2\pi/qL} \rho_q^{(-)\dagger}$ with \pm denoting the right and left Fermi points. According to the periodic boundary condition, a consistent choice for $M = M_R + M_L$ and $J = J_R + J_L$ is $M_R = J_R$, $M_L = -J_L$. Using the Bogoliubov transformation, the Hamiltonian can be easily diagonalized

$$H_B = \sum_{q>0} \tilde{v}_s q (a_q^\dagger a_q + \tilde{a}_q^\dagger \tilde{a}_q) + \frac{\hbar\pi}{2L} [\tilde{v}_N M^2 + \tilde{v}_J J^2], \quad (7)$$

where the Bogoliubov boson is given by $a_q^\dagger = b_q^\dagger \cosh \tilde{\varphi}_0 - \tilde{b}_q^\dagger \sinh \tilde{\varphi}_0$, $\tilde{a}_q^\dagger = \tilde{b}_q^\dagger \cosh \tilde{\varphi}_0 - b_q^\dagger \sinh \tilde{\varphi}_0$. The renormalized velocities are $\tilde{v}_s = |(v_s + U_1)^2 - U_1^2|^{1/2}$, $\tilde{v}_N =$

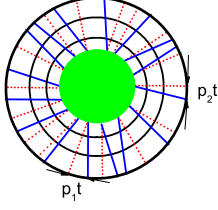


FIG. 5: (Color on-line) The sketch map of the image of the time-of-flight. Circles represent the positions of the atoms with the fastest radial velocity at the different flight time. The cross points between each blue solid lines and the circle is the position of these atoms. The red dotted lines are the reference radial lines.

$\tilde{v}_s e^{-2\tilde{\varphi}_0}$, and $\tilde{v}_J = \tilde{v}_s e^{2\tilde{\varphi}_0}$ with the controlling parameter $\tilde{\varphi}_0$ determined by

$$\tanh(2\tilde{\varphi}_0) = \frac{v_J - v_N - 2U_1/\hbar}{v_J + v_N + 2U_1/\hbar}. \quad (8)$$

Thus, the Luttinger liquid relation survives with the effective Luttinger liquid parameter

$$\lambda_{eff} = e^{-2\tilde{\varphi}_0}. \quad (9)$$

There is a restriction in U_1 for a given λ because $|\tanh 2\tilde{\varphi}_0| < 1$. For $\lambda > 0$, this holds if $U_1 > -\frac{1}{2}\lambda\hbar v_s$. Fig. 4 shows the Luttinger liquid parameter changes as interaction. An attractive U_1 suppresses λ_{eff} from λ while a repulsive one lifts λ_{eff} as expected. This exponent λ_{eff} may determine the non-universal exponents in the Luttinger liquid [22]. For example, the asymptotic single particle correlation function is proportional

to $x^{-\lambda_{eff}}$ so that the momentum distribution is given by $n(p) \sim C_1 - C_2 \text{sgn}(p - p_F)|p - p_F|^{(\lambda_{eff}-1)}$. In the limit $U_1 \rightarrow \infty$, the system goes an insulator state because $x^{-\lambda_{eff}} \rightarrow 0$ as $\lambda_{eff} \rightarrow \infty$.

The non-ideal gas theory does not work for the pure Lieb-Linger gas because eq.(9) is back to the free boson when $\lambda \rightarrow 0$. For $\lambda = 0$, the model is exactly soluble. We can use the exclusion gas theory with mutual statistics which was also developed in ref. [18]. It is a bosonization theory with a similar Hamiltonian to (7) with the effective Luttinger liquid parameter $\lambda_{eff} = [z(k_F^{(+)})z(k_F^{(-)})]^{-1}$ where $z(k)$ is given by the integration equation $z(k) = 1 + \int_{-k_F}^{k_F} \frac{dk'}{2\pi} \frac{U_1/2}{(U_1/2)^2 + (k-k')^2} z(k')$. The pseudo-Fermi momentum k_F is determined by the vanishing point of the dressed energy [2, 18] and $k_F^{(\pm)} = k_F \pm \epsilon$ for $\epsilon \rightarrow 0^+$. In the T-G limit ($U_1 \rightarrow \infty$), one finds $z(k_F^{(+)}) = 1$ and $z(k_F^{(-)}) = 2$, i.e., $\lambda_{eff} = 1/2$ [3].

Now, we discuss the possible experimental implication. $\lambda_{eff} - 1$ is the exponent of the one-dimensional momentum distribution, which can be measured by the absorption image of the time-flight. Keeping the inner wall potential of the cylinder and switching off the outer wall potential, the atom cloud will freely expand. The atoms with the fastest radial velocity will run along the blue lines in Fig. 5 if they have the different azimuthal momenta p . Counting the number of the different arc intervals (pt) at a given time t , one can draw out the momentum distribution of the cigar-like condensates before releasing. Then the exponent λ_{eff} can be determined. The system with $\lambda \neq 0$ is very different from $\lambda = 0$. This can be seen from the limit $U_1 \rightarrow \infty$. For the former, $\lambda_{eff} \rightarrow \infty$ and the system is an insulator while the latter has $\lambda_{eff} = 1/2$, the T-G gas state.

I thank S. M. Bhattacharjee to draw my attention to the renormalization group analysis to the C-S-L-L model. This work was supported in part by Chinese National Natural Science Foundation.

-
- [1] H. Bethe, Z. Physik **71**, 205 (1931).
 - [2] C. N. Yang and C. P. Yang, J. Math. Phys. **10**, 1115 (1969).
 - [3] E. H. Lieb and W. Liniger, Phys. Rev. **130**, 1605 (1963).
 - [4] F. Calogero, J. Math. Phys. **10**, 2191 and 2197 (1969).
 - [5] B. Sutherland, J. Math. Phys. **12**, 246 (1971); Phys. Rev. A **4**, 2019 (1971); **5**, 1372 (1972).
 - [6] W. Ketterle and N. J. vanDruten, Phys. Rev. A **54**, 656 (1996).
 - [7] L. Tonks, Phys. Rev. **50**, 955(1936); M. Girardeau, J. Math. Phys. **1**, 516 (1960).
 - [8] T. Kinoshita et al, Sciences **305**, 1125 (2004); B. Paredes et al, Nature **429**, 277 (2004).
 - [9] See e.g., J. F. van Diejen and L. Vinet (Eds.), *Calogero-*

- Moser-Sutherland Models: CRM Series in Mathematical Physics 2000 XXV*, (Springer, Berlin, Heidelberg, New York 2000) and references therein.
- [10] B. D. Simons, P. A. Lee, and B. L. Altshuler, Phys. Rev. Lett. **70**, 4122 (1993).
- [11] Y. Yu and Z. Y. Zhu, Comm. Theor. Phys. **29**, 351 (1998); Y. Yu, W. J. Zheng and Z. Y. Zhu, Phys. Rev. B **56**, 13279 (1997); W. J. Zheng and Y. Yu, Phys. Rev. Lett. **79**, 3242 (1997).
- [12] Y. Yu, e-preprint, cond-mat/0603340.
- [13] A. Griesmaier, J. Werner, S. Hensler, J. Stuhler, and T. Pfau, Phys. Rev. Lett. **94**, 160401(2005).
- [14] M. D. Girardeau, e-print-cond-mat/0604357.
- [15] R. Lipowsky and Th. M. Nieuwenhuizen, J. Phys. A **21**,

- L89 (1988). R. K. P. Zia, R. Lipowsky and D. M. Kroll, Am. J. Phys **56**, 160 (1988). S. M. Bhattacharjee, Phys. Rev. Lett. **76**, 4568 (1996); **83**, 2374 (1999).
- [16] M. Lässig, Phys. Rev. Lett. **77**, 526 (1996).
- [17] E. B. Kolomeisky and J. P. Straley, Phys. Rev. B **46**, 13942 (1994), and references therein.
- [18] Y. S. Wu and Y. Yu, Phys. Rev. Lett. **75**, 890 (1995); Y. S. Wu, Y. Yu and H. X. Yang, Nucl. Phys. B **604**, 551 (2001). Y. Yu, H. X. Yang and Y.S. Wu, e-preprint, cond-mat/9911141.
- [19] F. D. M. Haldane, Phys. Rev. Lett. **67**, 937 (1991).
- [20] Y. S. Wu, Phys. Rev. Lett. **73**, 922 (1994).
- [21] D. Bernard and Y. S. Wu, in Proc. 6th Nankai Workshop, eds. M. L. Ge and Y. S. Wu, World Scientific (1995).
- [22] F. D. M. Haldane, J. Phys. C **14**, 2585 (1981).
- [23] A. Luther and I. Peschel, Phys. Rev. B **9**, 2911 (1974); E. H. Lieb and D. C. Mattis, J. Math. Phys. **6**, 304(1965); J. M. Luttinger, J. Math. Phys. **4**, (1963); S. Tomonaga, Prog. Theor. Phys. **5**, 544 (1950).
- [24] S. Inouye et al, Nature (London) **392**, 151 (1998); J.L. Roberts et al, Phys. Rev. Lett. **86**, 4211 (2001).
- [25] S. Giovanazzi, A. Gorlitz, and T. Pfau, Phys. Rev. Lett. **89**, 130401 (2002).
- [26] L. Amico et al, Phys. Rev. Lett. **95**, 063201 (2005).
- [27] S. Yi and L. You, Phys. Rev. A **61**, 041604(R) (2000); L. Santos et al, Phys. Rev. Lett. **85**, 1791 (2000); K. Goral et al., Phys. Rev. A **61**, 051601(R) (2000).
- [28] N. Kawakami and S. K. Yang, Phys. Rev. Lett. **67**, 2493 (1991).